

# Supporting Information

Wang et al. 10.1073/pnas.1120193109

## SI Materials and Methods

**Cell Culture and Genotyping.** Mouse embryonic fibroblasts (MEFs) were prepared from day 13.5 embryos from XTV-ASPP2<sup>(+/Δ3)</sup> intercrosses. Genotyping was performed by PCR using the following primers:

- A: (5'-CCTCTCACAAAAGGAAATAACCTG-3')
- B: (5'-AGGAAAACCACCACCTTCAC-3')
- C: (5'-TACCCGCTCCATTGCTCAG-3')

Primers A and B amplify a 900-bp fragment from the ASPP2 WT allele, and primers B and C amplify a 1,100-bp fragment from the ASPP2 exon 3 KO allele (1). All animal procedures were approved by local ethical review and licensed by the UK Home Office. HKe-3 estrogen receptor (ER):HRAS V12 cells were a gift from Julian Downward (Signal Transduction Laboratory, Cancer Research UK London Research Institute, London, United Kingdom). Cells were cultured in DMEM supplemented with 10% FBS and antibiotics at 37 °C and 10% CO<sub>2</sub>.

**Plasmids and siRNAs.** pBabe-Puro HRAS V12 and pBabe-Bleo HRAS V12 were obtained from Julian Downward. Retroviral vectors for ASPP2-truncated fragments were generated by cloning truncated ASPP2 cDNA fragments into pLPCX-Puro. V5-tagged ASPP2 fragments were generated by cloning truncated ASPP2 cDNA fragments into pcDNA 3.1 TOPO (Invitrogen). pCI-neo-Apg5 was obtained from Addgene (2). ATG16 plasmid was generated by cloning ATG16 cDNA fragment into pcDNA 3.1. pKD-control-GFP (shRNA vector) and pKD-ATG5-GFP (hp2 and hp7, 2 independent shRNAs against mouse Atg5) constructs were obtained from Julian J. Lum (British Columbia Cancer Agency, University of Victoria, Victoria, BC, Canada). pBabe-GFP-ATG5 was obtained from Kevin Ryan (The Beatson Institute for Cancer Research, Glasgow, United Kingdom). pBabe-GFP-ATG5-K130R was generated by site-directed mutagenesis. The adenovirus expressing EGFP-LC3 was prepared using the AdEasy system as described previously (3). siRNA oligos against ASPP1, ASPP2, or iASPP were purchased from Dharmacon. Sequences are available from Dharmacon or on request. We used siGENOME RISC-Free siRNA (Dharmacon) as a negative control. Cells were transfected with the indicated siRNA oligos at a final concentration of 35 nM using Dharmafect 1 reagent (Dharmacon), according to the manufacturer's instructions.

**Western Blot Analysis.** Western blot (WB) analysis was performed with lysates prepared 6–8 d after transduction of RAS from subconfluent cells with urea buffer (8 M urea, 1 M thiourea, 0.5% CHAPS, 50 mM DTT, 24 mM spermine) or Nonidet P-40 lysis buffer (1% Nonidet P-40, 0.5% sodium deoxycholate in PBS) as described (4). Primary antibodies were from Santa Cruz (Beclin-1, ATG16, and p21), Cell Signaling (ATG3, ATG16, ATG5, phospho-S6, and S6), Upstate (RAS Clone 10), Abcam (GAPDH, tubulin, V5, and p19<sup>ARF</sup>), Cosmo Bio Co. (ATG5), Nanotools (LC3 and 5F10), ASPP1 (LX54.2), ASPP2 (DX54.10) (5), iASPP (LX49.3), and Novocastra (p53 CM-5). Signals were detected using an ECL detection system (GE Healthcare).

**Autophagic Activity Assays.** Autophagy was induced by several treatment regimes. To visualize rapamycin (Calbiochem)-induced autophagy, cells were infected with EGFP-LC3 adenovirus the day before treatment and then incubated in full medium containing 1% FBS in the presence of 50 μg/mL rapamycin for the

indicated periods. For endogenous LC3 analysis by WB, cells were treated with the regimes indicated in medium containing 10 μg/mL E-64d (Calbiochem) for 4 h, washed with cold PBS, and then lysed in PBS containing 2% Triton X-114 and protease inhibitors (Complete; Roche). After tumbling end over end at 4 °C for 1.5 h, tubes were spun at 13,000 × g for 10 min at 4 °C, a sample of the supernatant was precipitated with acetone, and pellets were dissolved in 50 mM Tris-Cl (pH 8.8) and 1% SDS. After normalizing protein concentrations, 50 μg of each sample was separated by SDS/PAGE, transferred onto a nitrocellulose membrane, and probed with anti-LC3 antibody. To inhibit autophagy, ASPP2<sup>(Δ3/Δ3)</sup> and ASPP2<sup>(+/+)</sup> MEFs transduced with pBabe-Puro HRAS V12 were infected twice with viral supernatants from pKD-Atg5-GFP (ATG5 shRNA) constructs overnight in the presence of 8 μg/mL polybrene. Forty-eight hours after infection, lysates were used for WB analysis.

**Measurement of the Degradation of Long-Lived Proteins.** Cells were plated onto 35-mm dishes and cultured in cysteine/methionine-free media containing 10 μCi of L-[<sup>35</sup>S]cysteine/methionine for 12 h at 37 °C. Unincorporated radioisotopes and degraded amino acids released from short-lived proteins were removed by rinsing three times with PBS. Cells were then chased with culture medium containing 10% FBS and 2 mM cold cysteine/methionine. After 6 h of incubation, at which time short-lived proteins were degraded, the chase medium was replaced with fresh medium with or without 50 μg/mL rapamycin. Incubation continued for an additional 5 h. The medium was harvested, and 10% trichloroacetic acid (TCA) was added. Samples were centrifuged at 12,000 × g for 10 min, and acid-soluble radioactivity was measured by liquid scintillation counting. Cells were fixed by adding 1 mL of 10% TCA directly to the culture dishes, washed with 10% TCA, and dissolved in 1 mL of 0.2 M NaOH. Radioactivity in the samples was then measured. The percentage of protein degradation was calculated by dividing the amount of acid-soluble radioactivity in the culture medium by the sum of acid-soluble and acid-precipitable radioactivities.

**Analysis of Senescence.** Analysis of senescence in cell culture was performed using a Senescence β-galactosidase staining kit (Cell Signaling) as described previously (4). To quantify senescence associated-β-galactosidase-positive findings, at least 200 cells were counted in random fields in each of the duplicated wells.

**Immunofluorescence.** Cells were fixed in 4% PBS-paraformaldehyde for 15 min; incubated in 0.2% Triton X-100 for 5 min and then in 0.2% fish skin gelatin in PBS for 10 min; and stained for 1 h with anti-LC3 (Nanotools), anti-ASPP2 (DX54.10), anti-ATG5 (Abgent), or anti-BrdU FITC antibody (BD Bioscience). Antibodies were used at a 1:100 dilution in 0.2% fish skin gelatin in PBS. Staining with the secondary antibody and TO-PRO-3 (Invitrogen) was then performed, followed by visualization under a fluorescence microscope. To quantify BrdU-positive findings, at least 200 cells were counted in random fields in each of the duplicated wells.

MitoSOX Red (Invitrogen) was used to detect reactive oxygen species levels in cells. In brief, MEFs were stained with MitoSOX (2.5 μM) for 20 min at 37 °C, protected from light, followed by fixation in 4% PBS-paraformaldehyde, and counterstained with TO-PRO-3. To quantify MitoSOX-positive findings, at least 200 cells were counted in random fields in each of the duplicated wells.

**Colony Formation Assay.** HRAS V12-expressing ASPP2<sup>(+/+)</sup> or ASPP2<sup>(Δ3/Δ3)</sup> MEFs were infected with shRNA against Atg5 (hp7) three times. For colony formation assay, 10,000 cells per well were seeded in six-well plates and kept in culture for 14 d. The colonies were stained with crystal violet and counted.

**Quantitative RT-PCR.** Real-time RT-PCR was performed using gene-specific primers (QuantiTect Primer Assays; Qiagen) for ATG5 or GAPDH with the QuantiTect SYBR Green RT-PCR Kit (Qiagen). Relative transcript levels of target genes were normalized to GAPDH mRNA levels.

**Immunoprecipitations.** Cells were lysed in NETN buffer [50 mM Tris (pH 8.0), 150 mM NaCl, 1 mM EDTA, 1% Nonidet P-40, protease inhibitor mixture (Roche)]. After lysis, extracts were precleared with 100 μL of protein G beads (50% slurry) for 60 min at 4 °C. For each immunoprecipitation, anti-ASPP2 (6), anti-ATG16 (Santa Cruz), or IgG was used, 25 μL of a 50% slurry of protein G beads was added, and samples were then rotated at

4 °C overnight. Beads were washed five times with 1 mL of NETN buffer, and 20 μL of 2× SDS loading buffer was added. Immunoprecipitations were analyzed by WB as indicated.

**In Vitro Translation and in Vitro Immunoprecipitation.** V5-tagged ASPP2 fragments, ATG5, and ATG16 were translated in vitro with cold methionine using the TNT T7 Quick Coupled Transcription/Translation System (Promega). The reticulocyte lysates containing indicated proteins were combined and incubated together for 1 h at 30 °C. The samples were precleared in 1 mL of PBS by rotating for 1 h at 4 °C with protein G Sepharose beads (Amersham Biosciences). Following removal of the beads, V5 antibody (AbD Serotec) or ATG16 antibody immobilized on protein G Sepharose beads was added to the binding reactions and rotated at 4 °C for 16 h. The beads were then washed with PBS. The bound proteins were released in SDS sample buffer and analyzed by SDS/PAGE/immunoblotting.

1. Vives V, et al. (2006) ASPP2 is a haploinsufficient tumor suppressor that cooperates with p53 to suppress tumor growth. *Genes Dev* 20:1262–1267.
2. Mizushima N, Sugita H, Yoshimori T, Ohsumi Y (1998) A new protein conjugation system in human. The counterpart of the yeast Apg12p conjugation system essential for autophagy. *J Biol Chem* 273:33889–33892.
3. Bampton ET, Goemans CG, Niranjana D, Mizushima N, Tolkovsky AM (2005) The dynamics of autophagy visualized in live cells: From autophagosome formation to fusion with endo/lysosomes. *Autophagy* 1(1):23–36.
4. Wang W, et al. (2002) Sequential activation of the MEK-extracellular signal-regulated kinase and MKK3/6-p38 mitogen-activated protein kinase pathways mediates oncogenic ras-induced premature senescence. *Mol Cell Biol* 22:3389–3403.
5. Samuels-Lev Y, et al. (2001) ASPP proteins specifically stimulate the apoptotic function of p53. *Mol Cell* 8:781–794.
6. Sottocornola R, et al. (2010) ASPP2 binds Par-3 and controls the polarity and proliferation of neural progenitors during CNS development. *Dev Cell* 19:126–137.

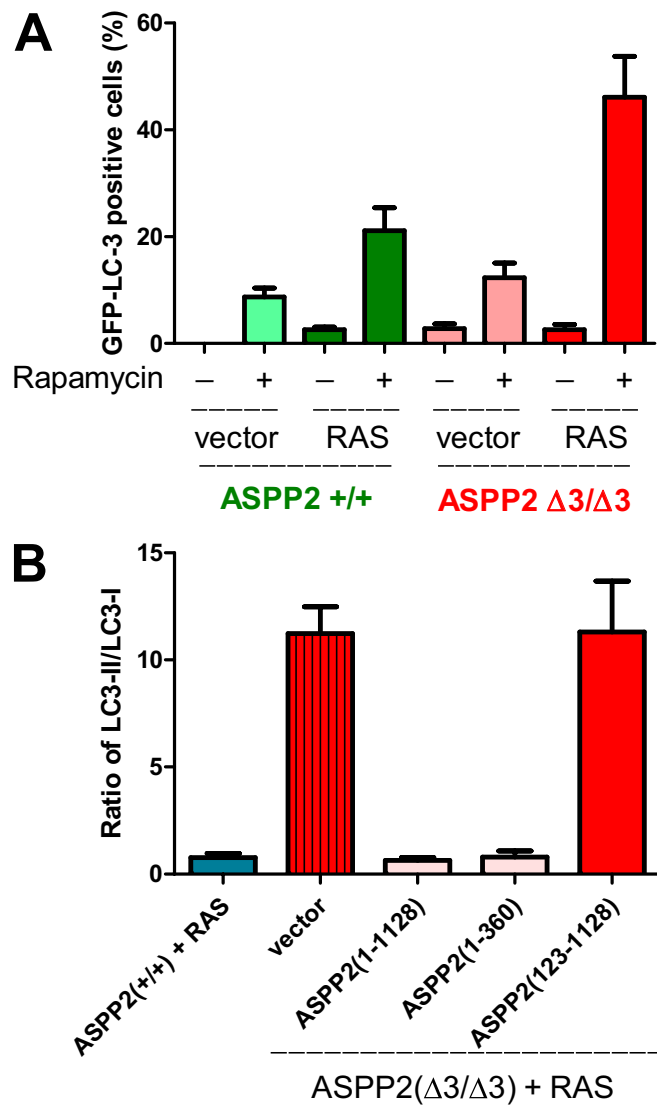


**Fig. S1.** ASPP2 inhibits oncogenic RAS-induced autophagy. (A) Graph shows the percentage of cells with at least a twofold increase of LC3-puncta compared with controls (as seen in Fig. 1F). Error bars indicate SD. (B) N terminus of ASPP2 is required and sufficient to inhibit oncogenic RAS-induced autophagy. The ratio of LC3-II against LC3-I (as seen in Fig. 1G) was calculated by densitometry. Error bars indicate SD.

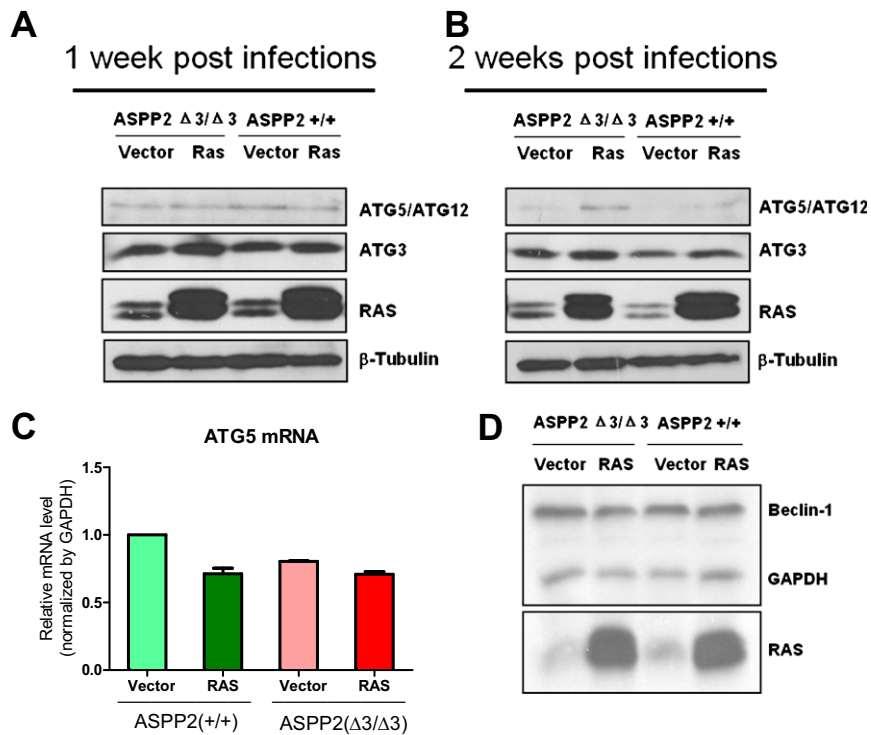


**Fig. 52.** Expression of autophagy components in indicated MEFs. (A and B) WB of ASPP2<sup>(+/+)</sup> or ASPP2<sup>( $\Delta 3/\Delta 3$ )</sup> MEF lysates, with or without HRAS V12 expression for 1 or 2 wk, shows effects on ATG5/ATG12 and ATG3 expression.  $\beta$ -Tubulin was used as a loading control. (C) Quantitative RT-PCR analysis of ATG5 mRNA levels in MEFs with the indicated treatments. (D) WB of ASPP2<sup>(+/+)</sup> or ASPP2<sup>( $\Delta 3/\Delta 3$ )</sup> MEF lysates, with or without HRAS V12 expression for 3 wk, shows effects on Beclin-1 expression. GAPDH was used as a loading control.

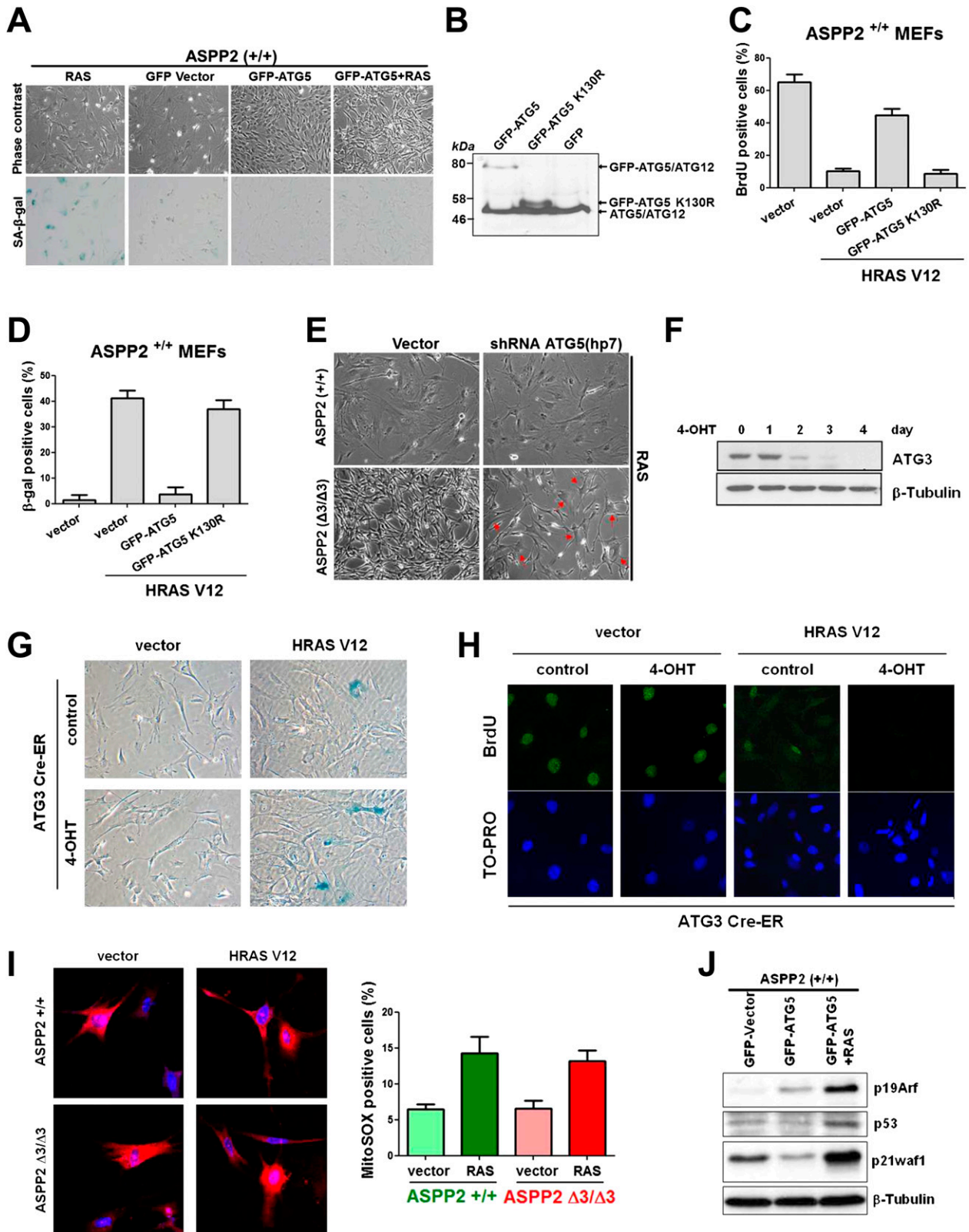


**Fig. 53.** High levels of autophagy bypass oncogenic RAS-induced senescence, whereas reduced levels of autophagy sensitize it. (A–D) Overexpression of ATG5, but not ATG5 K130R, prevents HRAS V12 from inducing senescence in ASP2<sup>(+/+)</sup> MEFs. (A) Phase contrast (*Upper*) and senescence associated-β-galactosidase (SA-β-gal) staining (*Lower*) images illustrate senescent cells. Images were taken with a ×20, air objective lens. (B) WB shows expression of exogenous GFP-ATG5/ATG12, GFP-ATG5 K130R, or endogenous ATG5/ATG12. (C) Graph shows the percentage of BrdU-positive cells with indicated infections (as seen in Fig. 3B). (D) Graph shows the percentage of SA-β-gal-positive cells with indicated infections (as seen in Fig. 3C). (E–H) Depletion of ATG5 or deletion of ATG3 accelerates RAS-induced senescence. (E) ASP2<sup>(+/+)</sup> or ASP2<sup>(Δ3/Δ3)</sup> MEFs with or without HRAS V12 expression were infected with shRNA constructs against mouse ATG5 (hp7) or control shRNA (Vector). Phase contrast images are shown to illustrate senescent cells as indicated by arrows. Images were taken with a ×20, air objective lens. (F) ASP2<sup>(+/+)</sup> MEFs were infected with shRNA constructs against mouse ATG3 (hp7) or control shRNA (Vector). Images were taken with a ×20, air objective lens. (G) ASP2<sup>(+/+)</sup> MEFs were infected with ATG3 Cre-ER or control Cre-ER. Images were taken with a ×20, air objective lens. (H) ASP2<sup>(+/+)</sup> MEFs were infected with ATG3 Cre-ER or control Cre-ER. Images were taken with a ×20, air objective lens. (I) ASP2<sup>(+/+)</sup> or ASP2<sup>(Δ3/Δ3)</sup> MEFs with or without HRAS V12 expression were infected with shRNA constructs against mouse ATG5 (hp7) or control shRNA (Vector). Images were taken with a ×20, air objective lens. (J) ASP2<sup>(+/+)</sup> MEFs were infected with GFP-Vector, GFP-ATG5, or GFP-ATG5 +RAS. Images were taken with a ×20, air objective lens.

objective lens. (F) WB shows that ATG3 is deleted following 4-hydroxytamoxifen (4-OHT; 200 nM) treatment in ATG3 Cre-ER MEFs. ATG3 Cre-ER MEFs with the indicated treatments were stained for SA- $\beta$ -gal activity (G) or BrdU incorporation (H) 1 wk after infection. Images for BrdU incorporation were taken with a  $\times 63$ , oil-immersion objective lens while images for SA- $\beta$ -gal activity were taken with a  $\times 20$ , air objective lens. (I) Reactive oxygen species (ROS) levels in ASPP2<sup>(+/+)</sup> or ASPP2<sup>( $\Delta 3/\Delta 3$ )</sup> MEFs infected with vector or HRAS V12. MitoSOX staining (red) in the images illustrates ROS-producing cells. Images were taken with a  $\times 63$ , oil-immersion objective lens. (Right) Graph shows the percentage of ROS-positive cells. At least 200 cells were counted in random fields in each of the duplicated wells to quantify MitoSOX-positive findings. (J) WB shows the expression of p19Arf, p53, and p21 in ASPP2<sup>(+/+)</sup> MEFs with the indicated treatments.  $\beta$ -Tubulin expression levels demonstrate equal loading.

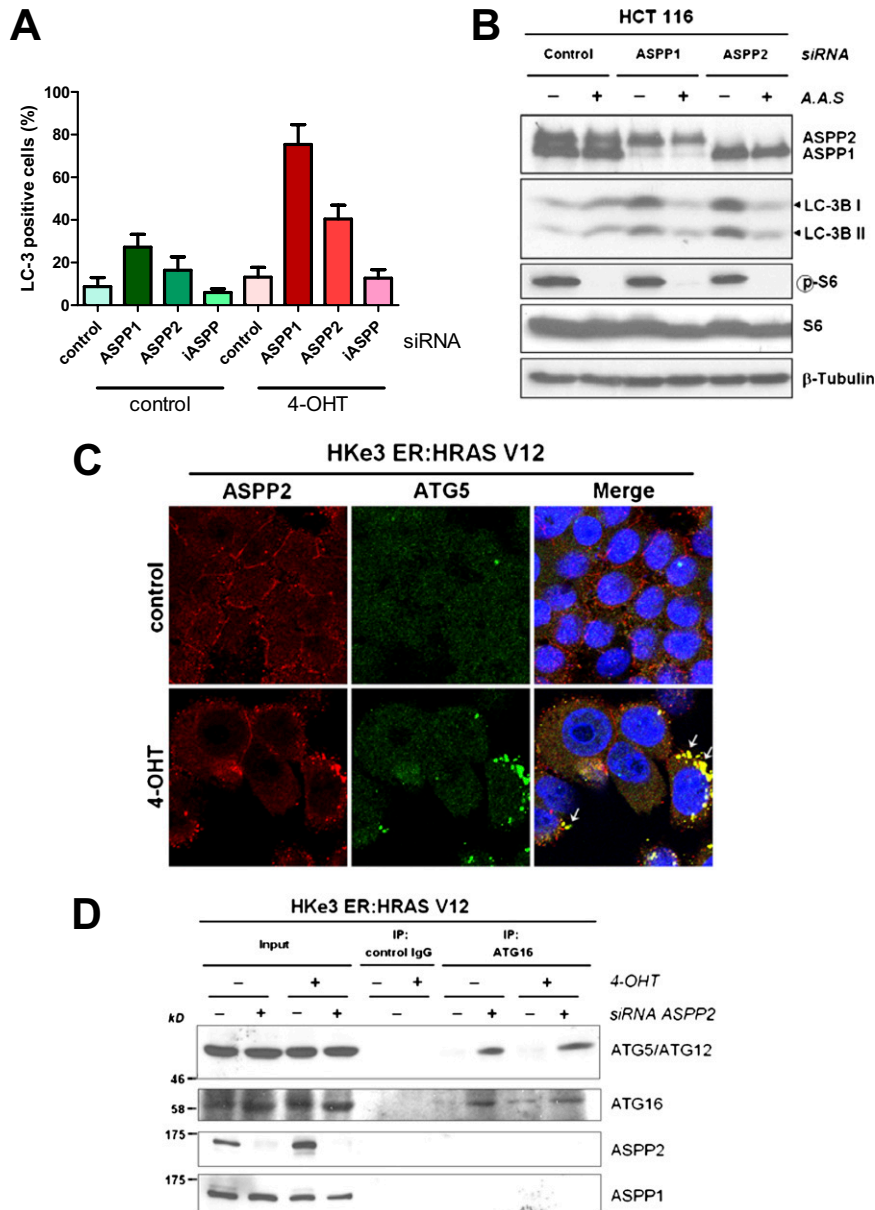


**Fig. S4.** ASPP2 inhibits autophagy by preventing ATG16 from complexing with ATG5/ATG12. (A) Graph shows the percentage of cells staining positive for LC3 puncta in HKe3 ER:HRAS V12 cells with the indicated ATG treatments (as seen in Fig. 4A). Error bars indicate SD. (B) HCT116 cells were transfected with the indicated siRNA for 4 d, followed by amino acid starvation (A.A.S) for 5 h. Indicated protein levels were detected by WB. Phospho-S6 (p-S6) levels indicate mammalian target of rapamycin activity. (C) ASPP2 colocalizes with ATG5 on RAS activation in HKe3 cells. Immunofluorescence staining of ASPP2 or ATG5 in HKe3 ER:HRAS V12 cells treated without (control) or with 4-hydroxytamoxifen (4-OHT) for 1 d. Arrows indicate colocalization. Images were taken with a  $\times 63$ , oil-immersion objective lens. (D) ASPP2 depletion enhances the binding between ATG16 and ATG5/ATG12 in HKe3 cells. HKe3 ER:HRAS V12 cells transfected with control siRNA or siRNA against ASPP2 for 3 d were treated with or without 100 nM 4-OHT for another day. Total cell lysates from HKe3 ER:HRAS V12 cells with the indicated treatments were immunoprecipitated with an anti-ATG16 antibody or control IgG. IP, immunoprecipitation.